

Transformer and Inductor design Handbook

Third Edition, Revised and Expanded

COLONEL WM. T. McLyman

Transformer and Inductor design Handbook

Third Edition, Revised and Expanded

COLONEL WM. T. McLYMAN

Kg Magnetics, Inc.

Idyllwild, California, U.S.A.

Although great care has been taken to provide accurate and current information, neither the author(s) nor the publisher, nor anyone else associated with this publication, shall be liable for any loss, damage, or liability directly or indirectly caused or alleged to be caused by this book. The material contained herein is not intended to provide specific advice or recommendations for any specific situation.

Trademark notice: Product or corporate names may be trademarks or registered trademarks and are used only for identification and explanation without intent to infringe.

Library of Congress Cataloging-in-Publication Data

A catalog record for this book is available from the Library of Congress.

ISBN: 0-8247-5393-3

This book is printed on acid-free paper.

Headquarters

Marcel Dekker, Inc. 270 Madison Avenue, New York, NY 10016, U.S.A. tel: 212-696-9000; fax: 212-685-4540

Distribution and Customer Service

Marcel Dekker, Inc. Cimarron Road, Monticello, New York 12701, U.S.A. tel: 800-228-1160; fax: 845-796-1772

Eastern Hemisphere Distribution

Marcel Dekker AG Hutgasse 4, Postfach 812, CH-4001 Basel, Switzerland tel: 41-61-260-6300; fax: 41-61-260-6333

World Wide Web

http://www.dekker.com

The publisher offers discounts on this book when ordered in bulk quantities. For more information, write to Special Sales/Professional Marketing at the headquarters address above.

Copyright © 2004 by Marcel Dekker, Inc. All Rights Reserved.

Neither this book nor any part may be reproduced or transmitted in any form or by any means, electronic or mechanical, including photocopying, microfilming, and recording, or by any information storage and retrieval system, without permission in writing from the publisher.

Current printing (last digit):

10 9 8 7 6 5 4 3 2 1

PRINTED IN THE UNITED STATES OF AMERICA

Copyright @ 2004 by Marcel Dekker, Inc. All Rights Reserved.

ELECTRICAL AND COMPUTER ENGINEERING

A Series of Reference Books and Textbooks

FOUNDING EDITOR

Marlin O. Thurston
Department of Electrical Engineering
The Ohio State University
Columbus, Ohio

- 1. Rational Fault Analysis, edited by Richard Saeks and S. R. Liberty
- Nonparametric Methods in Communications, edited by P. Papantoni-Kazakos and Dimitri Kazakos
- 3. Interactive Pattern Recognition, Yi-tzuu Chien
- 4. Solid-State Electronics, Lawrence E. Murr
- 5. Electronic, Magnetic, and Thermal Properties of Solid Materials, Klaus Schröder
- 6. Magnetic-Bubble Memory Technology, Hsu Chang
- 7. Transformer and Inductor Design Handbook, Colonel Wm. T. McLyman
- 8. Electromagnetics: Classical and Modern Theory and Applications, Samuel Seely and Alexander D. Poularikas
- 9. One-Dimensional Digital Signal Processing, Chi-Tsong Chen
- 10. Interconnected Dynamical Systems, Raymond A. DeCarlo and Richard Saeks
- 11. Modern Digital Control Systems, Raymond G. Jacquot
- 12. Hybrid Circuit Design and Manufacture, Roydn D. Jones
- Magnetic Core Selection for Transformers and Inductors: A User's Guide to Practice and Specification, Colonel Wm. T. McLyman
- 14. Static and Rotating Electromagnetic Devices, Richard H. Engelmann
- 15. Energy-Efficient Electric Motors: Selection and Application, John C. Andreas
- 16. Electromagnetic Compossibility, Heinz M. Schlicke
- 17. Electronics: Models, Analysis, and Systems, James G. Gottling
- 18. Digital Filter Design Handbook, Fred J. Taylor
- 19. Multivariable Control: An Introduction, P. K. Sinha
- 20. Flexible Circuits: Design and Applications, Steve Gurley, with contributions by Carl A. Edstrom, Jr., Ray D. Greenway, and William P. Kelly
- 21. Circuit Interruption: Theory and Techniques, Thomas E. Browne, Jr.
- 22. Switch Mode Power Conversion: Basic Theory and Design, K. Kit Sum
- 23. Pattern Recognition: Applications to Large Data-Set Problems, Sing-Tze Bow
- 24. Custom-Specific Integrated Circuits: Design and Fabrication, Stanley L. Hurst
- 25. Digital Circuits: Logic and Design, Ronald C. Emery
- Large-Scale Control Systems: Theories and Techniques, Magdi S. Mahmoud, Mohamed F. Hassan, and Mohamed G. Darwish
- 27. Microprocessor Software Project Management, Eli T. Fathi and Cedric V. W. Armstrong (Sponsored by Ontario Centre for Microelectronics)
- 28. Low Frequency Electromagnetic Design, Michael P. Perry
- Multidimensional Systems: Techniques and Applications, edited by Spyros G. Tzafestas
- AC Motors for High-Performance Applications: Analysis and Control, Sakae Yamamura

- 31. Ceramic Motors for Electronics: Processing, Properties, and Applications, edited by Relva C. Buchanan
- 32. Microcomputer Bus Structures and Bus Interface Design, Arthur L. Dexter
- 33. End User's Guide to Innovative Flexible Circuit Packaging, Jay J. Miniet
- 34. Reliability Engineering for Electronic Design, Norman B. Fugua
- Design Fundamentals for Low-Voltage Distribution and Control, Frank W. Kussy and Jack L. Warren
- 36. Encapsulation of Electronic Devices and Components, Edward R. Salmon
- 37. Protective Relaying: Principles and Applications, J. Lewis Blackburn
- 38. Testing Active and Passive Electronic Components, Richard F. Powell
- 39. Adaptive Control Systems: Techniques and Applications, V. V. Chalam
- Computer-Aided Analysis of Power Electronic Systems, Venkatachari Rajagopalan
- 41. Integrated Circuit Quality and Reliability, Eugene R. Hnatek
- 42. Systolic Signal Processing Systems, edited by Earl E. Swartzlander, Jr.
- 43. Adaptive Digital Filters and Signal Analysis, Maurice G. Bellanger
- 44. Electronic Ceramics: Properties, Configuration, and Applications, edited by Lionel M. Levinson
- 45. Computer Systems Engineering Management, Robert S. Alford
- 46. Systems Modeling and Computer Simulation, edited by Naim A. Kheir
- 47. Rigid-Flex Printed Wiring Design for Production Readiness, Walter S. Rigling
- 48. Analog Methods for Computer-Aided Circuit Analysis and Diagnosis, edited by Takao Ozawa
- Transformer and Inductor Design Handbook: Second Edition, Revised and Expanded, Colonel Wm. T. McLyman
- Power System Grounding and Transients: An Introduction, A. P. Sakis Meliopoulos
- 51. Signal Processing Handbook, edited by C. H. Chen
- 52. Electronic Product Design for Automated Manufacturing, H. Richard Stillwell
- 53. Dynamic Models and Discrete Event Simulation, William Delaney and Erminia Vaccari
- 54. FET Technology and Application: An Introduction, Edwin S. Oxner
- 55. Digital Speech Processing, Synthesis, and Recognition, Sadaoki Furui
- 56. VLSI RISC Architecture and Organization, Stephen B. Furber
- 57. Surface Mount and Related Technologies, Gerald Ginsberg
- Uninterruptible Power Supplies: Power Conditioners for Critical Equipment, David C. Griffith
- Polyphase Induction Motors: Analysis, Design, and Application, Paul L. Cochran
- 60. Battery Technology Handbook, edited by H. A. Kiehne
- Network Modeling, Simulation, and Analysis, edited by Ricardo F. Garzia and Mario R. Garzia
- 62. Linear Circuits, Systems, and Signal Processing: Advanced Theory and Applications, edited by Nobuo Nagai
- 63. High-Voltage Engineering: Theory and Practice, edited by M. Khalifa
- Large-Scale Systems Control and Decision Making, edited by Hiroyuki Tamura and Tsuneo Yoshikawa
- 65. Industrial Power Distribution and Illuminating Systems, Kao Chen
- 66. Distributed Computer Control for Industrial Automation, Dobrivoje Popovic and Vijay P. Bhatkar
- 67. Computer-Aided Analysis of Active Circuits, Adrian Ioinovici
- 68. Designing with Analog Switches, Steve Moore

- 69. Contamination Effects on Electronic Products, Carl J. Tautscher
- 70. Computer-Operated Systems Control, Magdi S. Mahmoud
- 71. Integrated Microwave Circuits, edited by Yoshihiro Konishi
- Ceramic Materials for Electronics: Processing, Properties, and Applications, Second Edition, Revised and Expanded, edited by Relva C. Buchanan
- 73. Electromagnetic Compatibility: Principles and Applications, David A. Weston
- 74. Intelligent Robotic Systems, edited by Spyros G. Tzafestas
- 75. Switching Phenomena in High-Voltage Circuit Breakers, edited by Kunio Nakanishi
- Advances in Speech Signal Processing, edited by Sadaoki Furui and M. Mohan Sondhi
- 77. Pattern Recognition and Image Preprocessing, Sing-Tze Bow
- Energy-Efficient Electric Motors: Selection and Application, Second Edition, John C. Andreas
- Stochastic Large-Scale Engineering Systems, edited by Spyros G. Tzafestas and Keigo Watanabe
- 80. Two-Dimensional Digital Filters, Wu-Sheng Lu and Andreas Antoniou
- 81. Computer-Aided Analysis and Design of Switch-Mode Power Supplies, Yim-Shu Lee
- 82. Placement and Routing of Electronic Modules, edited by Michael Pecht
- Applied Control: Current Trends and Modern Methodologies, edited by Spyros G. Tzafestas
- 84. Algorithms for Computer-Aided Design of Multivariable Control Systems, Stanoje Bingulac and Hugh F. VanLandingham
- 85. Symmetrical Components for Power Systems Engineering, J. Lewis Blackburn
- 86. Advanced Digital Signal Processing: Theory and Applications, Glenn Zelniker and Fred J. Taylor
- 87. Neural Networks and Simulation Methods, Jian-Kang Wu
- 88. Power Distribution Engineering: Fundamentals and Applications, James J. Burke
- 89. Modern Digital Control Systems: Second Edition, Raymond G. Jacquot
- 90. Adaptive IIR Filtering in Signal Processing and Control, Phillip A. Regalia
- 91. Integrated Circuit Quality and Reliability: Second Edition, Revised and Expanded, Eugene R. Hnatek
- Handbook of Electric Motors, edited by Richard H. Engelmann and William H. Middendorf
- 93. Power-Switching Converters, Simon S. Ang
- 94. Systems Modeling and Computer Simulation: Second Edition, Naim A. Kheir
- 95. EMI Filter Design, Richard Lee Ozenbaugh
- 96. Power Hybrid Circuit Design and Manufacture, Haim Taraseiskey
- 97. Robust Control System Design: Advanced State Space Techniques, Chia-Chi
 Tsui
- 98. Spatial Electric Load Forecasting, H. Lee Willis
- Permanent Magnet Motor Technology: Design and Applications, Jacek F. Gieras and Mitchell Wing
- 100. High Voltage Circuit Breakers: Design and Applications, Ruben D. Garzon
- 101. Integrating Electrical Heating Elements in Appliance Design, Thor Hegbom
- Magnetic Core Selection for Transformers and Inductors: A User's Guide to Practice and Specification, Second Edition, Colonel Wm. T. McLyman
- Statistical Methods in Control and Signal Processing, edited by Tohru Katayama and Sueo Sugimoto
- 104. Radio Receiver Design, Robert C. Dixon
- 105. Electrical Contacts: Principles and Applications, edited by Paul G. Slade

- 106. Handbook of Electrical Engineering Calculations, edited by Arun G. Phadke
- 107. Reliability Control for Electronic Systems, Donald J. LaCombe
- Embedded Systems Design with 8051 Microcontrollers: Hardware and Software, Zdravko Karakehayov, Knud Smed Christensen, and Ole Winther
- 109. Pilot Protective Relaying, edited by Walter A. Elmore
- High-Voltage Engineering: Theory and Practice, Second Edition, Revised and Expanded, Mazen Abdel-Salam, Hussein Anis, Ahdab El-Morshedy, and Roshdy Radwan
- 111. EMI Filter Design: Second Edition, Revised and Expanded, Richard Lee Ozenbaugh
- Electromagnetic Compatibility: Principles and Applications, Second Edition, Revised and Expanded, David Weston
- 113. Permanent Magnet Motor Technology: Design and Applications, Second Edition, Revised and Expanded, Jacek F. Gieras and Mitchell Wing
- High Voltage Circuit Breakers: Design and Applications, Second Edition, Revised and Expanded, Ruben D. Garzon
- High Reliability Magnetic Devices: Design and Fabrication, Colonel Wm. T. McLyman
- 116. Practical Reliability of Electronic Equipment and Products, Eugene R. Hnatek
- Electromagnetic Modeling by Finite Element Methods, João Pedro A. Bastos and Nelson Sadowski
- 118. Battery Technology Handbook: Second Edition, edited by H. A. Kiehne
- 119. Power Converter Circuits, William Shepherd and Li Zhang
- Handbook of Electric Motors: Second Edition, Revised and Expanded, edited by Hamid A. Toliyat and Gerald B. Kliman
- Transformer and Inductor Design Handbook: Third Edition, Revised and Expanded, Colonel Wm. T. McLyman

Additional Volumes in Preparation

Energy-Efficient Electric Motors: Third Edition, Revised and Expanded, Ali Emadi

To My Wife, Bonnie Copyright @ 2004 by Marcel Dekker, Inc. All Rights Reserved. NINTENDO-1012, p. 8 Nintendo v. Resonant

Foreword

Colonel McLyman is a well-known author, lecturer, and magnetic circuit designer. His previous books on transformer and inductor design, magnetic core characteristics, and design methods for converter circuits have been widely used by magnetics circuit designers.

In this book, Colonel McLyman has combined and updated the information found in his previous books. He has also added several new subjects such as rotary transformer design, planar transformer design, and planar construction. The author covers magnetic design theory with all of the relevant formulas along with complete information on magnetic materials and core characteristics. In addition, he provides real-world, step-by-step design examples.

This book is a must for engineers working in magnetic design. Whether you are working on high "rel" state-of-the-art design or high-volume or low-cost production, this book is essential. Thanks, Colonel, for a well-done, useful book.

Robert G. Noah Application Engineering Manager (Retired) Magnetics, Division of Spang and Company Pittsburgh, Pennsylvania, U.S.A.

Preface

I have had many requests to update *Transformer and Inductor Design Handbook*, because of the way power electronics has changed over the past few years. This new edition includes 21 chapters, with new topics such as: The forward converter, flyback converter, quiet converter, rotary transformers, and planar transformers, with even more design examples than the previous edition.

This book offers a practical approach, with design examples for design engineers and system engineers in the electronics and aerospace industries. Transformers are found in virtually all electronic circuits. This book can easily be used to design lightweight, high-frequency aerospace transformers or low-frequency commercial transformers. It is, therefore, a design manual.

The conversion process in power electronics requires the use of transformers, components that frequently are the heaviest and bulkiest item in the conversion circuit. Transformer components also have a significant effect on the overall performance and efficiency of the system. Accordingly, the design of such transformers has an important influence on overall system weight, power conversion efficiency, and cost. Because of the interdependence and interaction of these parameters, judicious trade-offs are necessary to achieve design optimization.

Manufacturers have, for years, assigned numeric codes to their cores to indicate their power-handling ability. This method assigns to each core a number called the area product, A_p , that is the product of its window area, W_a , and core cross-section area, A_c . These numbers are used by core suppliers to summarize dimensional and electrical properties in their catalogs. The product of the window area, W_a , and the core area, A_c , gives the area Product, A_p , a dimension to the fourth power. I have developed a new equation for the power-handling ability of the core, the core geometry, K_g . K_g has a dimension to the fifth power. This new equation provides engineers with faster and tighter control of their design. It is a relatively new concept, and magnetic core manufacturers are now beginning to include it in their catalogs.

Because of their significance, the area product, A_p , and the core geometry, K_g , are treated extensively in this handbook. A great deal of other information is also presented for the convenience of the designer. Much of the material is in tabular form to assist the designer in making the trade-offs best suited for a particular application in a minimum amount of time.

Designers have used various approaches in arriving at suitable transformer and inductor designs. For example, in many cases a rule of thumb used for dealing with current density is that a good working level is 1000 circular mils per ampere. This is satisfactory in many instances; however, the wire size used to meet this requirement may produce a heavier and bulkier inductor than desired or required. The information

presented here will make it possible to avoid the use of this and other rules of thumb, and to develop a more economical and better design. While other books are available on electronic transformers, none of them seems to have been written with the user's viewpoint in mind. The material in this book is organized so that the student engineer or technician—starting at the beginning of the book and continuing through the end—will gain a comprehensive knowledge of the state of the art in transformer and inductor design.

No responsibility is assumed by the author or the publisher for any infringement of patent or other rights of third parties that may result from the use of circuits, systems, or processes described or referred to in this handbook.

Acknowledgments

In gathering the material for this book, I have been fortunate in having the assistance and cooperation of several companies and many colleagues. I wish to express my gratitude to all of them. The list is too long to mention them all. However, there are some individuals and companies whose contributions have been especially significant. Colleagues who have retired from Magnetics include Robert Noah and Harry Savisky, who helped so greatly with the editing of the final draft. Other contributions were made by my colleagues at Magnetics, Lowell Bosley and his staff for sending up-to-date catalogs and sample cores. I would like to thank colleagues at Micrometals Corp., Jim Cox and Dale Nicol, and George Orenchak of TSC International. I would like to give special thanks to Richard (Oz) Ozenbaugh of Linear Magnetics Corp. for his assistance in the detailed derivations of many of the equations and his efforts in checking the design examples. I also give special thanks to Steve Freeman of Rodon Products, Inc., for building and testing the magnetics components used in the design examples.

I am also grateful to: Dr. Vatche Vorperian of Jet Propulsion Laboratory (JPL) for his help in generating and clarifying equations for the Quiet Converter; Jerry Fridenberg of Fridenberg Research, Inc., for modeling circuits on his SPICE program; Dr. Gene Wester of JPL for his input; and Kit Sum for his assistance in the energy-storage equations. I also thank the late Robert Yahiro for his help and encouragement over the years.

Colonel Wm. T. McLyman

About the Author

Colonel Wm. T. McLyman recently retired as a Senior Member of the Avionics Equipment Section of the Jet Propulsion Laboratory (JPL) affiliated with the California Institute of Technology in Pasadena, California. He has 47 years of experience in the field of Magnetics, and holds 14 United States Patents on magnetics-related concepts. Through his 30 years at JPL, he has written over 70 JPL Technical Memorandums, New Technology Reports, and Tech-Briefs on the subject of magnetics and circuit designs for power conversion. He has worked on projects for NASA including the Pathfinder Mission to Mars, Cassini, Galileo, Magellan, Viking, Voyager, MVM, Hubble Space Telescope, and many others.

He has been on the lecture circuit for over 20 years speaking in the United States, Canada, Mexico, and Europe on the design and fabrication of magnetic components. He is known as a recognized authority in magnetic design. He is currently the President of his own company, Kg Magnetics, Inc., which specializes in power magnetics design.

He recently completed a book entitled, *High Reliability Magnetic Devices: Design and Fabrication* (Marcel Dekker, Inc.). He also markets, through Kg Magnetics, Inc., a magnetics design and analysis software computer program called "Titan" for transformers and inductors (see Figure 1). This program operates on Windows 95, 98, 2000, and NT.

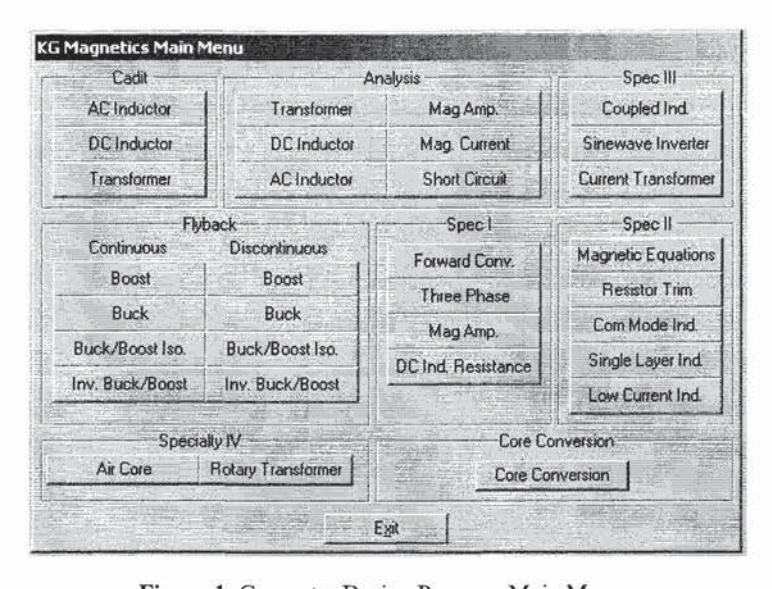


Figure 1. Computer Design Program Main Menu.

Colonel Wm. T. McLyman, (President)

Kg Magnetics, Inc.

Idyllwild, California 92549, U.S.A.

www.kgmagnetics.com; colonel@kgmagnetics.com

Contents Foreword Robert G. Noah Preface About the Author Symbols Chapter 1 Fundamentals of Magnetics Chapter 2 Magnetic Materials and Their Characteristics Chapter 3 Magnetic Cores Chapter 4 Window Utilization, Magnet Wire, and Insulation Chapter 5 Transformer Design Trade-Offs Chapter 6 Transformer-Inductor Efficiency, Regulation, and Temperature Rise Chapter 7 Power Transformer Design Chapter 8 DC Inductor Design Using Gapped Cores Chapter 9 DC Inductor Design Using Powder Cores Chapter 10 AC Inductor Design Chapter 11 Constant Voltage Transformer (CVT) Chapter 12 Three-Phase Transformer Design Chapter 13

Copyright © 2004 by Marcel Dekker, Inc. All Rights Reserved.

Input Filter Design

Flyback Converter, Transformer Design

Forward Converter, Transformer Design, and Output Inductor Design

Chapter 14

Chapter 15

Chapter 16

Current Transformer Design

Chapter 17

Winding Capacitance and Leakage Inductance

Chapter 18

Quiet Converter Design

Chapter 19

Rotary Transformer Design

Chapter 20

Planar Transformers

Chapter 21

Derivations for the Design Equations

Symbols

α	regulation, %
A_c	effective cross section of the core, cm ²
$A_{\mathfrak{p}}$	area product, cm4
\mathbf{A}_{t}	surface area of the transformer, cm ²
$A_{\rm w}$	wire area, cm ²
$A_{w(B)}$	bare wire area, cm ²
$A_{w(I)}$	insulated wire area, cm ²
A_{wp}	primary wire area, cm ²
A_{ws}	secondary wire area, cm ²
A-T	amp turn
AWG	American Wire Gage
В	flux, tesla
B_{ac}	alternating current flux density, tesla
ΔB	change in flux, tesla
B_{dc}	direct current flux density, tesla
B_{m}	flux density, tesla
B_{max}	maximum flux density, tesla
B_{o}	operating peak flux density, tesla
B_{pk}	peak flux density, tesla
$\mathbf{B}_{\mathbf{r}}$	residual flux density, tesla
B_{s}	saturation flux density, tesla
C	capacitance
C_n	new capacitance
C_p	lumped capacitance
CM	circular mils
D_{AWG}	wire diameter, cm
D _(min)	minimum duty ratio
$D_{(max)}$	maximum duty ratio
D_x	dwell time duty ratio
E	voltage
E_{Line}	line to line voltage
E_{Phase}	line to neutral voltage
Energy	energy, watt-second

ESR equivalent series resistance efficiency η f frequency, Hz F fringing flux factor magneto-motive force, mmf F_{m} F.L. full load G winding length, cm density, in grams-per-cm² γ 3 skin depth, cm magnetizing force, oersteds H H_c magnetizing force required to return flux to zero, oersteds ΔH delta magnetizing force, oersteds H_o operating peak magnetizing force H_s magnetizing force at saturation, oersteds Ι current, amps I_c charge current, amps ΔI delta current, amps dc current, amps I_{in} input current, amps input line current, amps I_{Line} I_{Phase} input phase current, amps I_{m} magnetizing current, amps I_{o} load current, amps maximum load current, amps I_{o(max)} minimum load current, amps I_{o(min)} I_p primary current, amps I, secondary current, amps I_{s(Phase)} secondary phase current, amps $I_{s(Line)}$ secondary line current, amps J current density, amps per cm2 Kc copper loss constant Kc quasi-voltage waveform factor electrical coefficient K_e

K_f	waveform coefficient
K_g	core geometry coefficient, cm5
K_j	constant related to current density
K_s	constant related to surface area
K_u	window utilization factor
K_{up}	primary window utilization factor
K_{us}	secondary window utilization factor
K_{vol}	constant related to volume
$K_{\rm w}$	constant related to weight
L	inductance, henry
L_c	open circuit inductance, henry
L_p	primary inductance, henry
1	is a linear dimension
$L_{(crt)}$	critical inductance
λ	density, grams per cm ³
$l_{\rm g}$	gap, cm
l_m	magnetic path length, cm
l_t	total path length, cm
mks	meters-kilogram-seconds
MLT	mean length turn, cm
mmf	magnetomotive force, F _m
MPL	magnetic path length, cm
mW/g	milliwatts-per-gram
μ	permeability
$\mu_{\rm i}$	initial permeability
μ_{Δ}	incremental permeability
μ_{m}	core material permeability
μ_{o}	permeability of air
μ_{r}	relative permeability
$\mu_{\boldsymbol{e}}$	effective permeability
n	turns ratio
N	turns
N.L.	no load

 N_L inductor turns N_n new turns N_p primary turns N_s secondary turns P watts P_{cu} copper loss, watts P_{fe} core loss, watts P_g gap loss, watts ф magnetic flux P_{in} input power, watts P_L inductor copper loss, watts Po output power, watts P_p primary copper loss, watts P_s secondary copper loss, watts P_{Σ} total loss (core and copper), watts P_t total apparent power, watts P_{VA} primary volt-amps R resistance, ohms Rac ac resistance, ohms R_{cu} copper resistance, ohms R_{dc} de resistance, ohms Re equivalent core loss (shunt) resistance, ohms R_g reluctance of the gap R_{m} reluctance R_{mt} total reluctance R_o load resistance, ohms $R_{o(R)}$ reflected load resistance, ohms reflected load resistance, ohms $R_{\text{in}(\text{equiv})}$ R_p primary resistance, ohms R_R ac/dc resistance ratio R_s secondary resistance, ohms

> total resistance, ohms resistivity, ohm-cm

 R_t

ρ

S_1	conductor area/wire area
S_2	wound area/usable window
S_3	usable window area/window area
S_4	usable window area/usable window area + insulation area
S_{np}	number of primary strands
S_{ns}	number of secondary strands
S_{VA}	secondary volt-amps
T	total period, seconds
t_{off}	off time, seconds
t _{on}	on time, seconds
$t_{\mathbf{w}}$	dwell time, seconds
$T_{\mathbf{r}}$	temperature rise, °C
U	multiplication factor
VA	volt-amps
V_{ac}	applied voltage, volts
V_c	control voltage, volts
$V_{c(pk)}$	peak voltage, volts
V_d	diode voltage drop, volts
V_{in}	input voltage, volts
$V_{\text{in}(\text{max})}$	maximum input voltage, volts
$V_{\text{in}(\text{min})}$	minimum input voltage, volts
V_n	new voltage, volts
V_o	output voltage, volts
V_p	primary voltage, volts
$V_{p(rms)}$	primary rms voltage, volts
$V_{s(LL)}$	secondary line to line voltage, volts
$V_{s(LN)}$	secondary line to neutral voltage, volts
$V_{r(pk)}$	peak ripple voltage
V_s	secondary voltage, volts
ΔV_{CC}	capacitor voltage, volts
ΔV_{CR}	capacitor ESR voltage, volts
ΔV_{p}	delta primary voltage, volts
ΔV_s	delta secondary voltage, volts

W watts

W/kg watts-per-kilogram W_a window area, cm^2

 W_{ap} primary window area, cm² W_{as} secondary window area, cm² $W_{a(eff)}$ effective window area, cm²

 W_{tcu} copper weight, grams W_{tfe} iron weight, grams

X_L inductive reactance, ohms

Chapter 1

Fundamentals of Magnetics

Copyright @ 2004 by Marcel Dekker, Inc. All Rights Reserved.

Introduction

Considerable difficulty is encountered in mastering the field of magnetics because of the use of so many different systems of units – the centimeter-gram-second (cgs) system, the meter-kilogram-second (mks) system, and the mixed English units system. Magnetics can be treated in a simple way by using the cgs system. There always seems to be one exception to every rule and that is permeability.

Magnetic Properties in Free Space

A long wire with a dc current, I, flowing through it, produces a circulatory magnetizing force, H, and a magnetic field, B, around the conductor, as shown in Figure 1-1, where the relationship is:

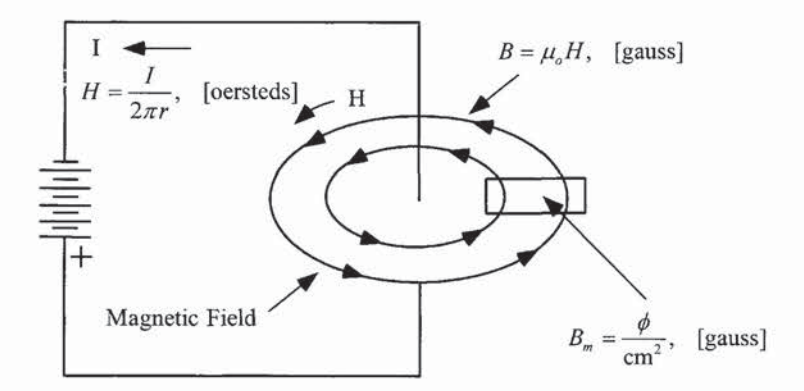


Figure 1-1. A Magnetic Field Generated by a Current Carrying Conductor.

The direction of the line of flux around a straight conductor may be determined by using the "right hand rule" as follows: When the conductor is grasped with the right hand, so that the thumb points in the direction of the current flow, the fingers point in the direction of the magnetic lines of force. This is based on so-called conventional current flow, not the electron flow.

When a current is passed through the wire in one direction, as shown in Figure 1-2(a), the needle in the compass will point in one direction. When the current in the wire is reversed, as in Figure 1-2(b), the needle will also reverse direction. This shows that the magnetic field has polarity and that, when the current I, is reversed, the magnetizing force, H, will follow the current reversals.

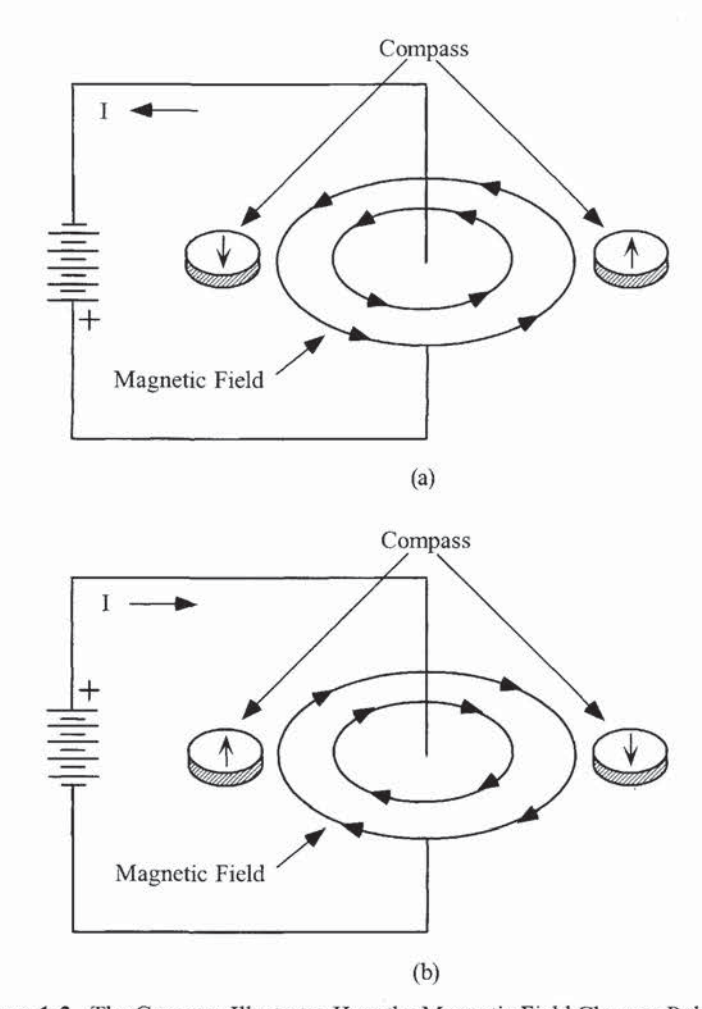


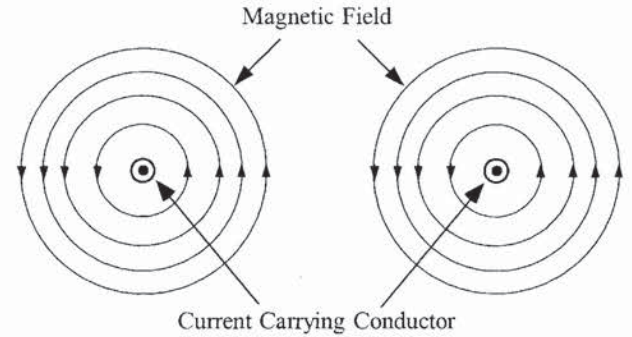
Figure 1-2. The Compass Illustrates How the Magnetic Field Changes Polarity.

Intensifying the Magnetic Field

When a current passes through a wire, a magnetic field is set up around the wire. If the conductors, as shown in Figure 1-3, carrying current in the same direction are separated by a relatively large distance, the magnetic fields generated will not influence each other. If the same two conductors are placed close to each other, as shown in Figure 1-4, the magnetic fields add, and the field intensity doubles.

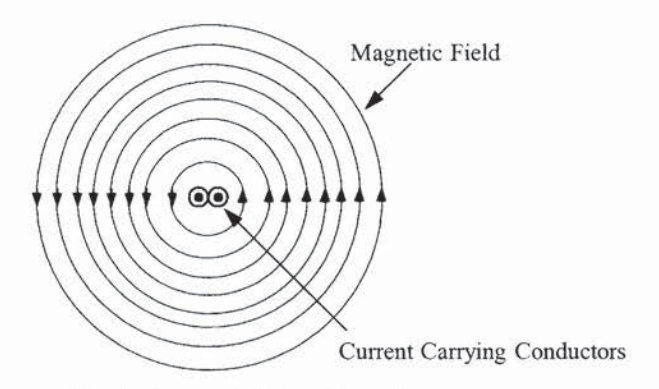
$$\gamma = \frac{B^2}{8\pi \mu}$$
, [energy density] [1-1]

If the wire is wound on a dowel, its magnetic field is greatly intensified. The coil, in fact, exhibits a magnetic field exactly like that of a bar magnet, as shown in Figure 1-5. Like the bar magnet, the coil has a north pole and a neutral center region. Moreover, the polarity can be reversed by reversing the current, I, through the coil. Again, this demonstrates the dependence of the magnetic field on the current direction.



Large distance between conductors.

Figure 1-3. Magnetic Fields Produced Around Spaced Conductors.



Conductors are in Close Proximity

Figure 1-4. Magnetic Fields Produced Around Adjacent Conductors.

The magnetic circuit is the space in which the flux travels around the coil. The magnitude of the flux is determined by the product of the current, I, and the number of turns, N, in the coil. The force, NI, required to create the flux is magnetomotive force (mmf). The relationship between flux density, B, and magnetizing force, H, for an air-core coil is shown in Figure 1-6. The ratio of B to H is called the permeability, μ , and for this air-core coil the ratio is unity in the cgs system, where it is expressed in units of gauss per oersteds, (gauss/oersteds).

$$\mu_o = 1$$

$$B = \mu_o H$$
[1-2]

If the battery, in Figure 1-5, were replaced with an ac source, as shown in Figure 1-7, the relationship between B and H would have the characteristics shown in Figure 1-8. The linearity of the relationship between B and H represents the main advantage of air-core coils. Since the relationship is linear, increasing H increases B, and therefore the flux in the coil, and, in this way, very large fields can be produced with large currents. There is obviously a practical limit to this, which depends on the maximum allowable current in the conductor and the resulting rise.

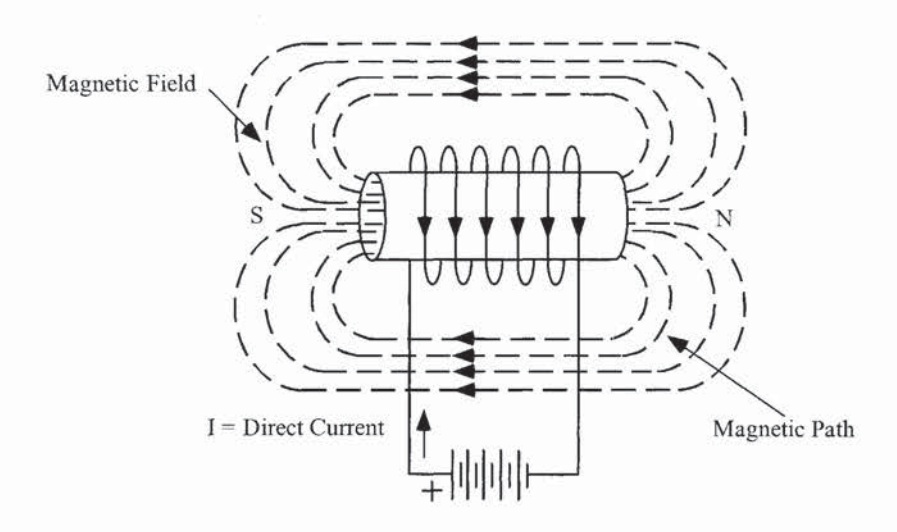


Figure 1-5. Air-Core Coil with dc excitation

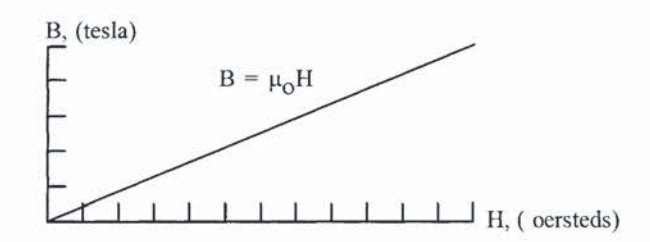


Figure 1-6. Relationship Between B and H with dc Excitation.

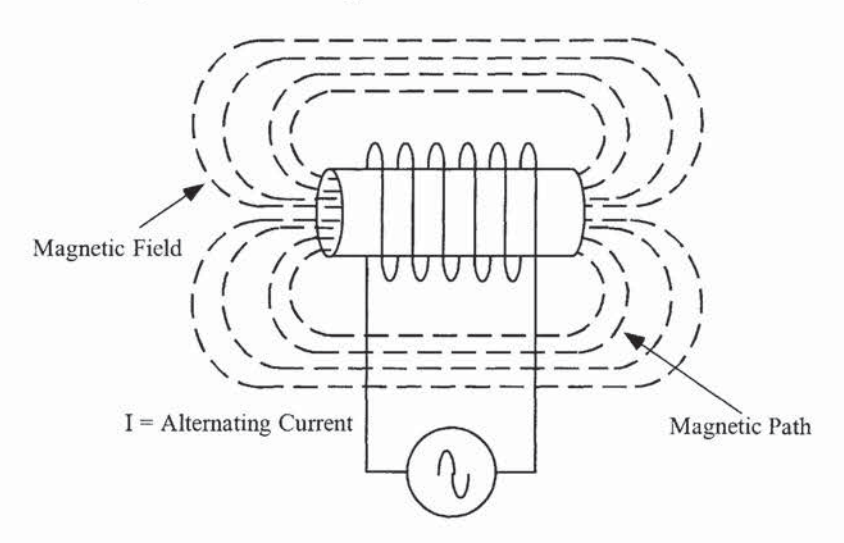


Figure 1-7. Air-Core Coil Driven from an ac Source.

Fields of the order of 0.1 tesla are feasible for a 40° C temperature rise above room ambient temperature. With super cooled coils, fields of 10 tesla have been obtained.

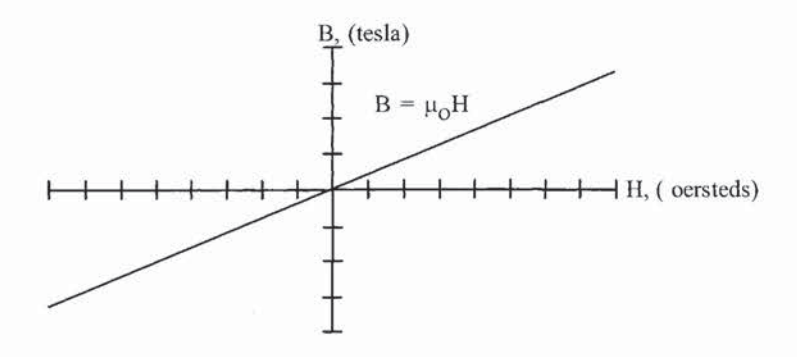


Figure 1-8. Relationship Between B and H with ac Excitation.

Simple Transformer

A transformer in its simplest form is shown in Figure 1-9. This transformer has two air coils that share a common flux. The flux diverges from the ends of the primary coil in all directions. It is not concentrated or confined. The primary is connected to the source and carries the current that establishes a magnetic field. The other coil is open-circuited. Notice that the flux lines are not common to both coils. The difference between the two is the leakage flux; that is, leakage flux is the portion of the flux that does not link both coils.

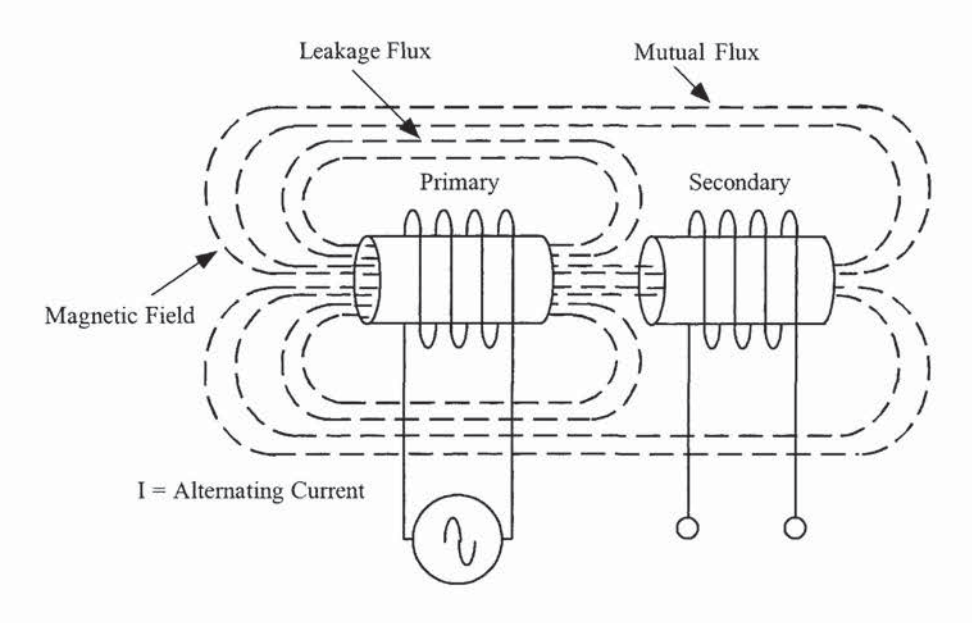


Figure 1-9. The Simplest Type of Transformer.

Magnetic Core

Most materials are poor conductors of magnetic flux; they have low permeability. A vacuum has a permeability of 1.0, and nonmagnetic materials, such as air, paper, and copper have permeabilities of the same order. There are a few materials, such as iron, nickel, cobalt, and their alloys that have high permeability, sometimes ranging into the hundreds of thousands. To achieve an improvement over the aircoil, as shown in Figure 1-10, a magnetic core can be introduced, as shown in Figure 1-11. In addition to its high permeability, the advantages of the magnetic core over the air-core are that the magnetic path length (MPL) is well-defined, and the flux is essentially confined to the core, except in the immediate vicinity of the winding. There is a limit as to how much magnetic flux can be generated in a magnetic material before the magnetic core goes into saturation, and the coil reverts back to an air-core, as shown in Figure 1-12.

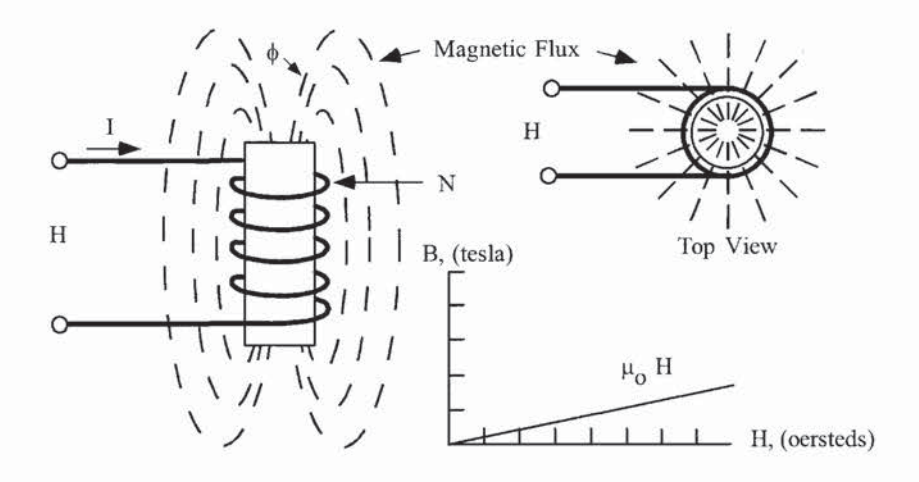


Figure 1-10. Air-Core Coil Emitting Magnetic Flux when Excited.

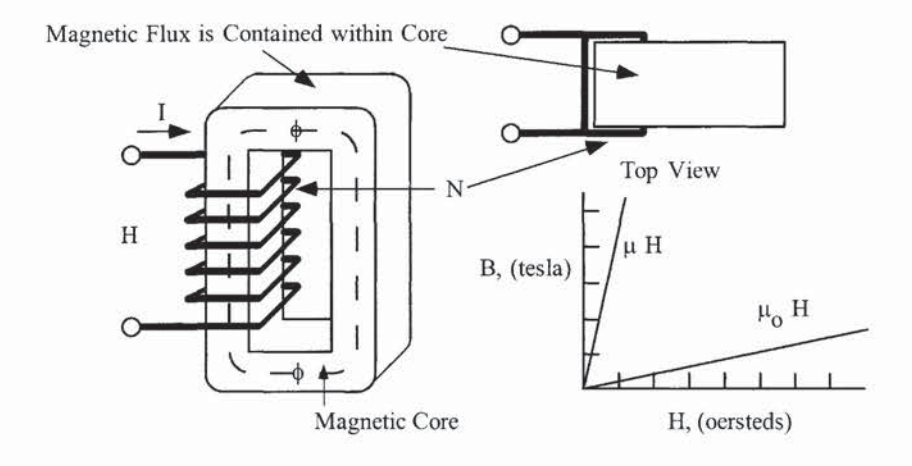


Figure 1-11. Introduction of a Magnetic Core.

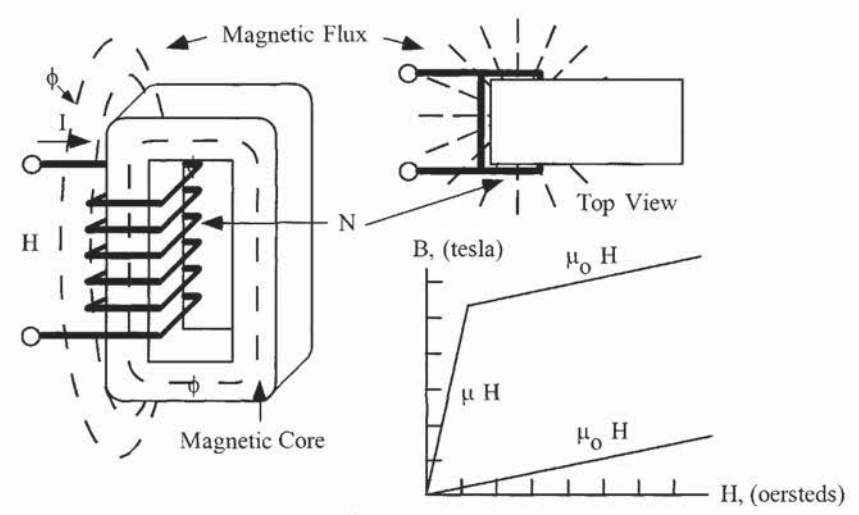


Figure 1-12. Excited Magnetic Core Driven into Saturation.

Fundamental Characteristics of a Magnetic Core

The effect of exciting a completely demagnetized, ferromagnetic material, with an external magnetizing force, H, and increasing it slowly, from zero, is shown in Figure 1-13, where the resulting flux density is plotted as a function of the magnetizing force, H. Note that, at first, the flux density increases very slowly up to point A, then, increases very rapidly up to point B, and then, almost stops increasing. Point B is called the knee of the curve. At point C, the magnetic core material has saturated. From this point on, the slope of the curve is:

$$\frac{B}{H} = 1$$
, [gauss/oersteds] [1-3]

The coil is now behaving as if it had an air-core. When the magnetic core is in hard saturation, the coil has the same permeability as air, or unity. Following the magnetization curve in Figure 1-14, Figures 1-15 through Figures 1-16 show how the flux in the core is generated from the inside of the core to the outside until the core saturates.

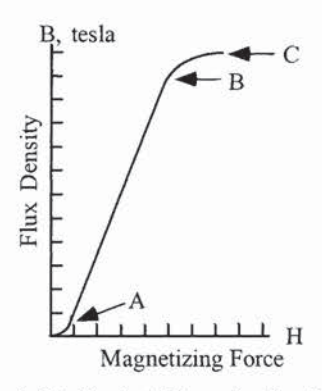


Figure 1-13. Typical Magnetization Curve.

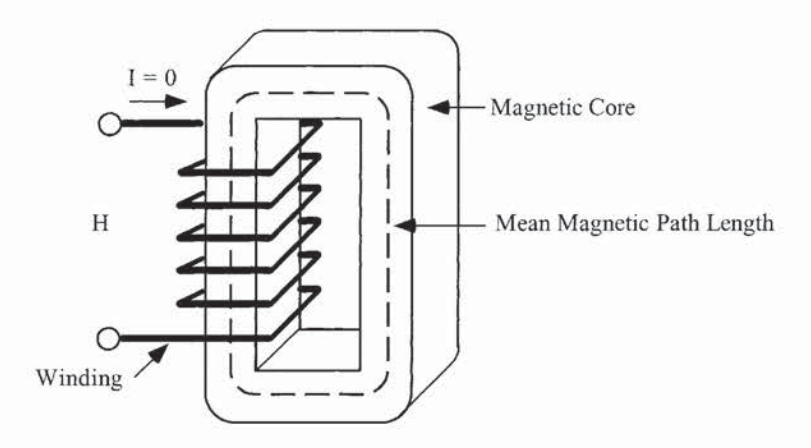


Figure 1-14. Magnetic Core with Zero Excitation.

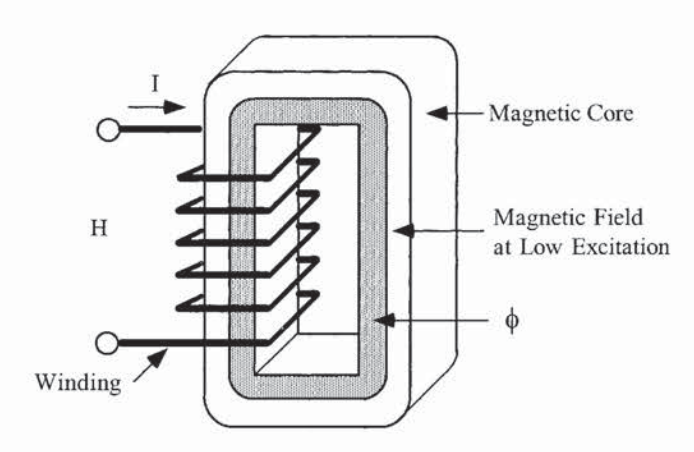


Figure 1-15. Magnetic Core with Low Excitation.

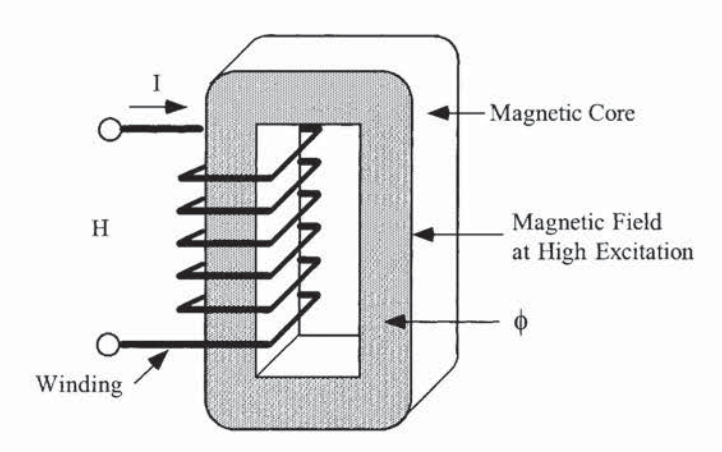


Figure 1-16. Magnetic Core with High Excitation.

Hysteresis Loop (B-H Loop)

An engineer can take a good look at the hysteresis loop and get a first order evaluation of the magnetic material. When the magnetic material is taken through a complete cycle of magnetization and demagnetization, the results are as shown in Figure 1-17. It starts with a neutral magnetic material, traversing the B-H loop at the origin X. As H is increased, the flux density B increases along the dashed line to the saturation point, B_s. When H is now decreased and B is plotted, B-H loop transverses a path to B_r, where H is zero and the core is still magnetized. The flux at this point is called remanent flux, and has a flux density, B_r.

The magnetizing force, H_s , is now reversed in polarity to give a negative value. The magnetizing force required to reduce the flux B_r to zero is called the coercive force, H_c . When the core is forced into saturation, the retentivity, B_{rs} , is the remaining flux after saturation, and coercivity, H_{cs} , is the magnetizing force required to reset to zero. Along the initial magnetization curve at point X, the dashed line, in Figure 1-17, B increases from the origin nonlinearly with H, until the material saturates. In practice, the magnetization of a core in an excited transformer never follows this curve, because the core is never in the totally demagnetized state, when the magnetizing force is first applied.

The hysteresis loop represents energy lost in the core. The best way to display the hysteresis loop is to use a dc current, because the intensity of the magnetizing force must be so slowly changed that no eddy currents are generated in the material. Only under this condition is the area inside the closed B-H loop indicative of the hysteresis. The enclosed area is a measure of energy lost in the core material during that cycle. In ac applications, this process is repeated continuously and the total hysteresis loss is dependent upon the frequency.

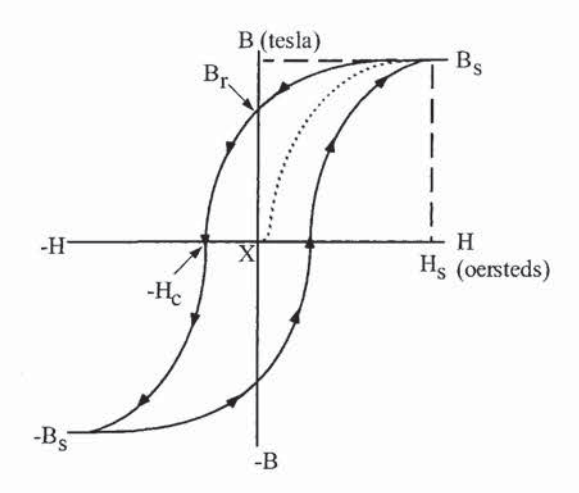


Figure 1-17. Typical Hysteresis Loop.

Permeability

In magnetics, permeability is the ability of a material to conduct flux. The magnitude of the permeability at a given induction is the measure of the ease with which a core material can be magnetized to that induction. It is defined as the ratio of the flux density, B, to the magnetizing force, H. Manufacturers specify permeability in units of gauss per oersteds.

Permeability =
$$\frac{B}{H}$$
, $\left[\frac{\text{gauss}}{\text{oersteds}}\right]$ [1-4]

The absolute permeability, μ_0 in cgs units is unity 1 (gauss per oersteds) in a vacuum.

cgs:
$$\mu_o = 1$$
, $\left[\frac{\text{gauss}}{\text{oersteds}}\right] = \left[\frac{\text{tesla}}{\text{oersteds}}\right]$ [1-5]
mks: $\mu_o = 0.4\pi \left(10^{-8}\right)$, $\left[\frac{\text{henrys}}{\text{meter}}\right]$

When B is plotted against H, as in Figure 1-18, the resulting curve is called the magnetization curve. These curves are idealized. The magnetic material is totally demagnetized and is then subjected to gradually increasing magnetizing force, while the flux density is plotted. The slope of this curve, at any given point gives the permeability at that point. Permeability can be plotted against a typical B-H curve, as shown in Figure 1-19. Permeability is not constant; therefore, its value can be stated only at a given value of B or H.

There are many different kinds of permeability, and each is designated by a different subscript on the symbol μ .

- μ_o Absolute permeability, defined as the permeability in a vacuum.
- μ_i Initial permeability is the slope of the initial magnetization curve at the origin. It is measured at very small induction, as shown in Figure 1-20.
- μ_{Δ} Incremental permeability is the slope of the magnetization curve for finite values of peak-topeak flux density with superimposed dc magnetization as shown in Figure 1-21.
- μ_e Effective permeability. If a magnetic circuit is not homogeneous (i.e., contains an air gap), the effective permeability is the permeability of hypothetical homogeneous (ungapped) structure of the same shape, dimensions, and reluctance that would give the inductance equivalent to the gapped structure.
- μ_r Relative permeability is the permeability of a material relative to that of free space.
- μ_n Normal permeability is the ratio of B/H at any point of the curve as shown in Figure 1-22.
- μ_{max} Maximum permeability is the slope of a straight line drawn from the origin tangent to the curve at its knee as shown in Figure 1-23.
- μ_p Pulse permeability is the ratio of peak B to peak H for unipolar excitation.
- μ_m Material permeability is the slope of the magnetization curve measure at less than 50 gauss as shown in Figure 1-24.

Permeability 1-13

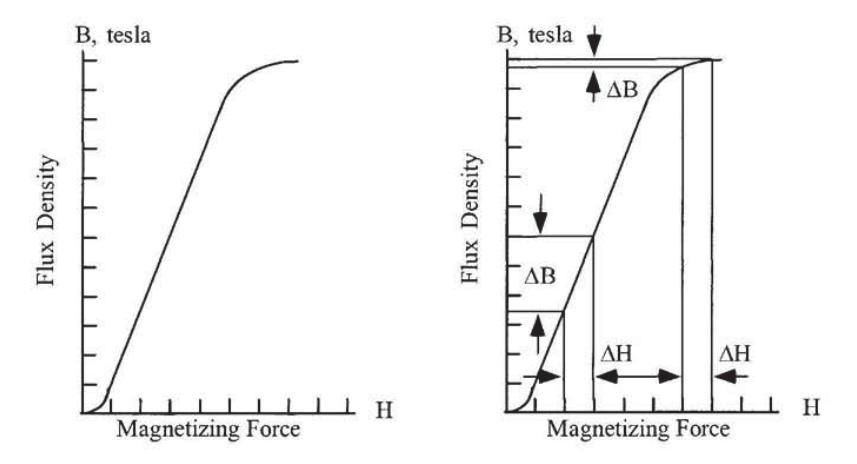


Figure 1-18. Magnetizing Curve.

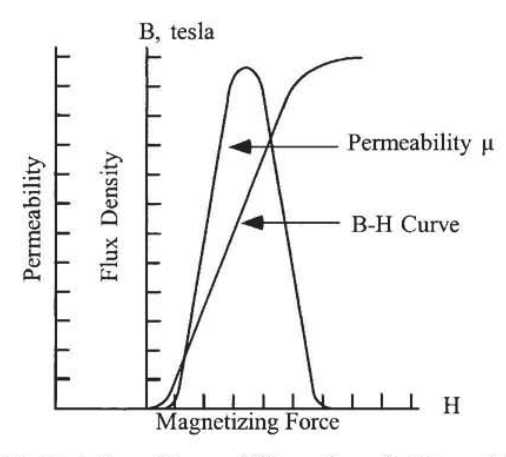


Figure 1-19. Variation of Permeability μ along the Magnetizing Curve.

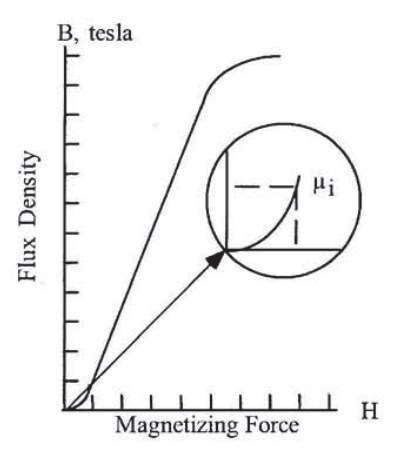


Figure 1-20. Initial Permeability.

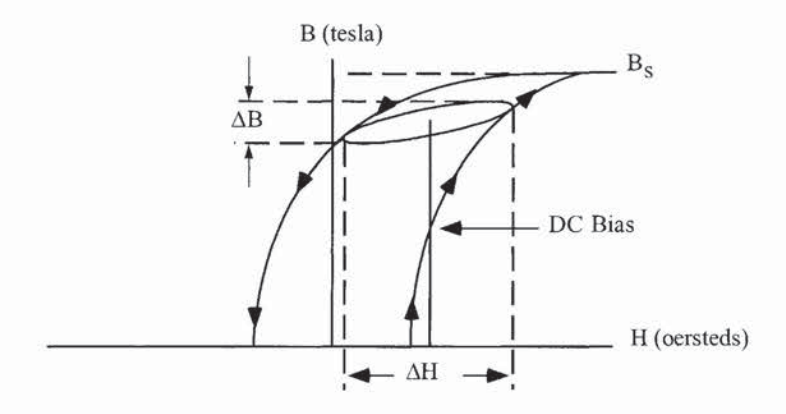


Figure 1-21. Incremental Permeability.

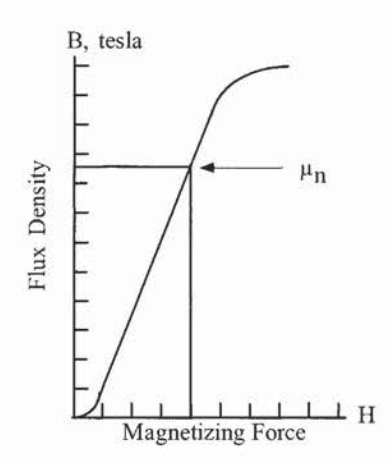


Figure 1-22. Normal Permeability.

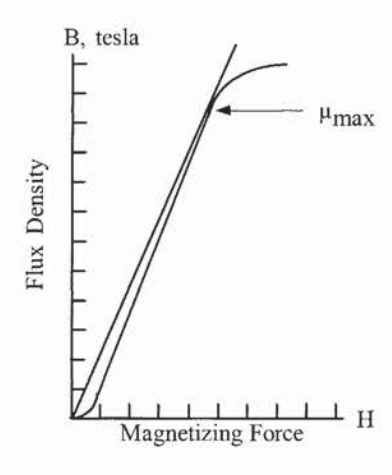


Figure 1-23. Maximum Permeability.

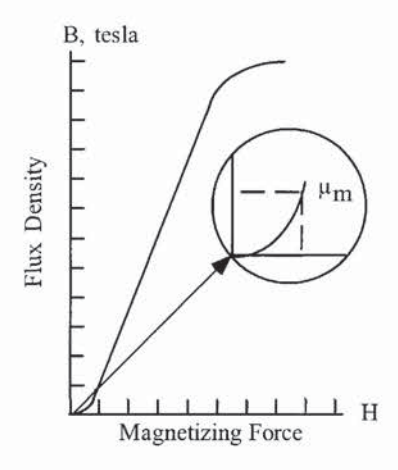


Figure 1-24. Material Permeability.

Magnetomotive Force (mmf) and Magnetizing Force (H)

There are two force functions commonly encountered in magnetics: magnetomotive force, mmf, and magnetizing force, H. Magnetomotive force should not be confused with magnetizing force; the two are related as cause and effect. Magnetomotive force is given by the equation:

$$mmf = 0.4\pi NI$$
, [gilberts] [1-6]

Where, N is the number of turns and I is the current in amperes. Whereas mmf is the force, H is a force field, or force per unit length:

$$H = \frac{\text{mmf}}{\text{MPL}}, \quad \left[\frac{\text{gilberts}}{\text{cm}} = \text{oersteds} \right] \quad [1-7]$$

Substituting,

$$H = \frac{0.4\pi NI}{\text{MPL}}, \text{ [oersteds]} \quad [1-8]$$

Where, MPL = magnetic path length in cm.

If the flux is divided by the core area, Ac, we get flux density, B, in lines per unit area:

$$B = \frac{\phi}{A_c}, \quad [\text{gauss}] \quad [1-9]$$

The flux density, B, in a magnetic medium, due to the existence of a magnetizing force H, depends on the permeability of the medium and the intensity of the magnetic field:

$$B = \mu H$$
, [gauss] [1-10]

The peak, magnetizing current, Im, for a wound core can be calculated from the following equation:

$$I_m = \frac{H_o(MPL)}{0.4\pi N}$$
, [amps] [1-11]

Where H_0 is the field intensity at the peak operating point. To determine the magnetizing force, H_0 , use the manufacturer's core loss curves at the appropriate frequency and operating flux density, B_0 , as shown in Figure 1-25.

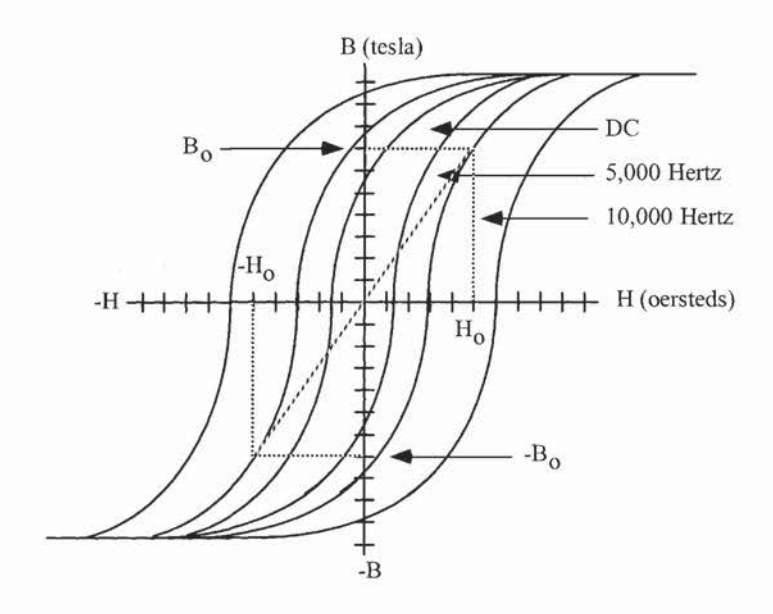


Figure 1-25. Typical B-H Loops Operating at Various Frequencies.

Reluctance

The flux produced in a given material by magnetomotive force (mmf) depends on the material's resistance to flux, which is called reluctance, $R_{\rm m}$. The reluctance of a core depends on the composition of the material and its physical dimension and is similar in concept to electrical resistance. The relationship between mmf, flux, and magnetic reluctance is analogous to the relationship between emf, current, and resistance, as shown in Figure 1-26.

emf
$$(E) = IR = \text{Current x Resistance}$$

mmf $(F_m) = \Phi R_m = \text{Flux x Reluctance}$ [1-12]

A poor conductor of flux has a high magnetic resistance, R_m. The greater the reluctance, the higher the magnetomotive force that is required to obtain a given magnetic field.

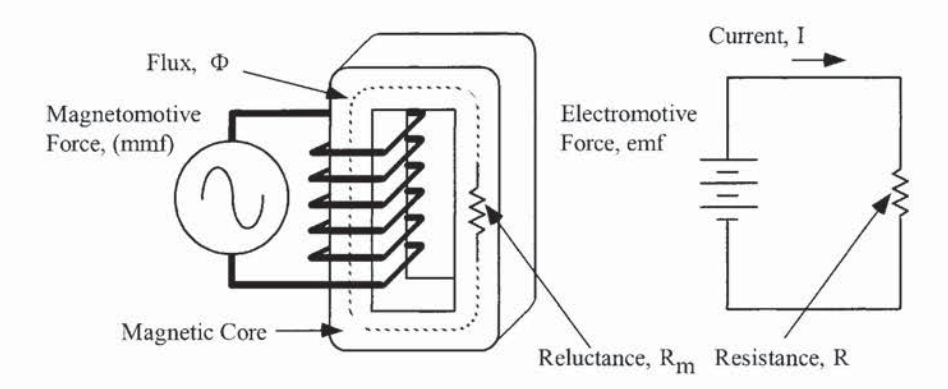


Figure 1-26. Comparing Magnetic Reluctance and Electrical Resistance.

The electrical resistance of a conductor is related to its length I, cross-sectional area A_w , and specific resistance ρ , which is the resistance per unit length. To find the resistance of a copper wire of any size or length, we merely multiply the resistivity by the length, and divide by the cross-sectional area:

$$R = \frac{\rho l}{A_{w}}, \quad [\text{ohms}] \quad [1-13]$$

In the case of magnetics, $1/\mu$ is analogous to ρ and is called reluctivity. The reluctance R_m of a magnetic circuit is given by:

$$R_m = \frac{\text{MPL}}{\mu_r \, \mu_o \, A_c} \quad [1-14]$$

Where MPL, is the magnetic path length, cm.

A_c is the cross-section of the core, cm².

 μ_{r} is the permeability of the magnetic material.

 μ_o is the permeability of air.

A typical magnetic core is shown in Figure 1-27 illustrating the magnetic path length MPL and the cross-sectional area, A_c, of a C core.

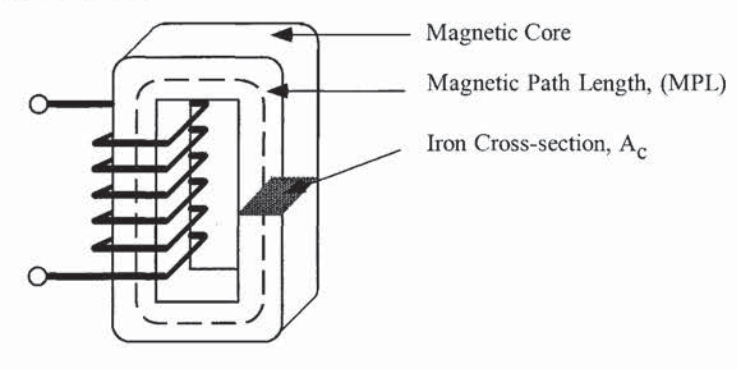


Figure 1-27. Magnetic Core Showing the Magnetic Path Length (MPL) and Iron Cross-section Ac-

Air Gap

A high permeability material is one that has a low reluctance for a given magnetic path length (MPL) and iron cross-section, A_c. If an air gap is included in a magnetic circuit as shown in Figure 1-28, which is otherwise composed of low reluctivity material like iron, almost all of the reluctance in the circuit will be at the gap, because the reluctivity of air is much greater than that of a magnetic material. For all practical purposes, controlling the size of the air gap controls the reluctance.

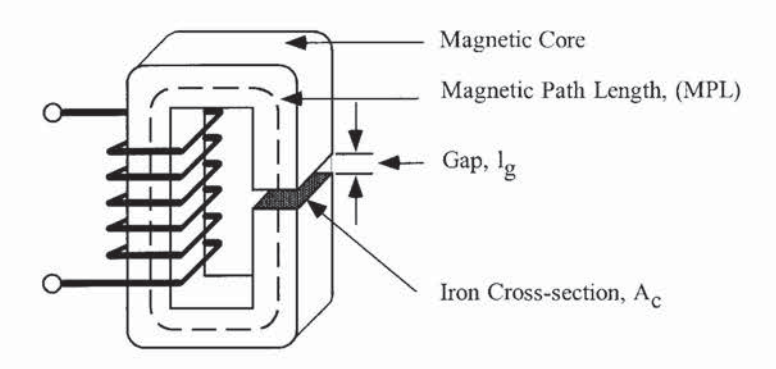


Figure 1-28. A Typical Magnetic Core with an Air Gap.

An example can best show this procedure. The total reluctance of the core is the sum of the iron reluctance and the air gap reluctance, in the same way that two series resistors are added in an electrical circuit. The equation for calculating the air gap reluctance, $R_{\rm g}$, is basically the same as the equation for calculating the reluctance of the magnetic material, $R_{\rm m}$. The difference is that the permeability of air is 1 and the gap length, $l_{\rm g}$, is used in place of the magnetic path length (MPL). The equation is as follows:

$$R_g = \left(\frac{1}{\mu_o}\right) \left(\frac{l_g}{A_c}\right) \quad [1-15]$$

But, since $\mu_0 = 1$, the equation simplifies to:

$$R_g = \frac{l_g}{A_c} \quad [1-16]$$

Where:

lg is the gap length, cm.

 A_c is the cross-section of the core, cm².

 μ_o is the permeability of air.

The total reluctance, R_{mt}, for the core shown in Figure 1-28 is therefore:

$$R_{mt} = R_m + R_g$$

$$R_{mt} = \frac{MPL}{\mu_r \, \mu_o \, A_c} + \frac{l_g}{\mu_o \, A_c}$$
[1-17]

Where μ_r is the relative permeability, which is used exclusively with magnetic materials.

$$\mu_r = \frac{\mu}{\mu_o} = \frac{B}{\mu_o H}, \quad \left[\frac{\text{gauss}}{\text{oersteds}}\right] \quad [1-18]$$

The magnetic material permeability, μ_m , is given by:

$$\mu_m = \mu_r \, \mu_o \quad [1-19]$$

The reluctance of the gap is higher than that of the iron even when the gap is small. The reason is because the magnetic material has a relatively high permeability, as shown in Table 1-1. So the total reluctance of the circuit depends more on the gap than on the iron.

Table 1-1. Material Permeability

Material Permeability, μ _m	
Material Name	Permeability
Iron Alloys	0.8K to 25K
Ferrites	0.8K to 20K
Amorphous	0.8K to 80K

After the total reluctance, R_t , has been calculated, the effective permeability, μ_e , can be calculated.

$$R_{mr} = \frac{l_r}{\mu_e A_c}$$

$$[1-20]$$

$$l_r = l_a + \text{MPL}$$

Where l_t is the total path length and μ_e is the effective permeability.

 $R_{mt} = \frac{l_t}{\mu_0 A_c} = \frac{l_g}{\mu_0 A_c} + \frac{\text{MPL}}{\mu_0 \mu_0 A_c}$ [1-21]

Simplifying yields:

 $\frac{l_t}{\mu_e} = \frac{l_g}{\mu_o} + \frac{\text{MPL}}{\mu_o \, \mu_r} \quad [1-22]$

Then:

$$\mu_e = \frac{l_r}{\frac{l_s}{\mu_o} + \frac{\text{MPL}}{\mu_o \mu_r}}$$

$$\mu_e = \frac{l_g + \text{MPL}}{\frac{l_g}{\mu_o} + \frac{\text{MPL}}{\mu_o}}$$

If $l_g <<$ MPL, multiply both sides of the equation by $(\mu_r \mu_o \ MPL)/$ ($\mu_r \mu_o \ MPL$).

$$\mu_e = \frac{\mu_o \, \mu_r}{1 + \mu_r \left(\frac{l_g}{\text{MPL}}\right)} \quad [1-24]$$

The classic equation is:

$$\mu_e = \frac{\mu_m}{1 + \mu_m \left(\frac{l_g}{\text{MPL}}\right)} \quad [1-25]$$

Introducing an air gap, l_g , to the core cannot correct for the dc flux, but can sustain the dc flux. As the gap is increased, so is the reluctance. For a given magnetomotive force, the flux density is controlled by the gap.

Controlling the dc Flux with an Air Gap

There are two similar equations used to calculate the dc flux. The first equation is used with powder cores. Powder cores are manufactured from very fine particles of magnetic materials. This powder is coated with an inert insulation to minimize eddy currents losses and to introduce a distributed air gap into the core structure.

$$\mu_r = \mu_e$$

$$B_{de} = \left(\mu_r\right) \left(\frac{0.4\pi NI}{\text{MPL}}\right), \quad \text{[gauss]} \quad [1-26]$$

$$\mu_r = \frac{\mu_m}{1 + \mu_m \left(\frac{l_g}{\text{MPL}}\right)}$$

The second equation is used, when the design calls for a gap to be placed in series with the magnetic path length (MPL), such as a ferrite cut core, a C core, or butt stacked laminations.

$$\mu_r = \mu_c$$

$$B_{dc} = \left(\mu_r\right) \left(\frac{0.4\pi NI}{\text{MPL}}\right), \quad \text{[gauss]} \quad [1-27]$$

Substitute (MPL μ_m) /(MPL μ_m) for 1:

$$\mu_r = \frac{\mu_m}{1 + \mu_m \left(\frac{l_g}{\text{MPL}}\right)} = \frac{\mu_m}{\frac{\text{MPL}\mu_m}{\text{MPL}\mu_m} + \mu_m \left(\frac{l_g}{\text{MPL}}\right)} \quad [1-28]$$

Then, simplify:

$$\mu_r = \frac{\text{MPL}}{\frac{\text{MPL}}{\mu_m} + l_g} \quad [1-29]$$

$$B_{dc} = \left(\frac{\text{MPL}}{\frac{\text{MPL}}{\mu_m} + I_g}\right) \left(\frac{0.4\pi NI}{\text{MPL}}\right), \text{ [gauss]} \quad [1-30]$$

Then, simplify:

$$B_{dc} = \frac{0.4\pi NI}{l_g + \frac{\text{MPL}}{\mu_-}}, \text{ [gauss]} \quad [1-31]$$

Types of Air Gaps

Basically, there are two types of gaps used in the design of magnetic components: bulk and distributed. Bulk gaps are maintained with materials, such as paper, Mylar, or even glass. The gapping materials are designed to be inserted in series with the magnetic path to increase the reluctance, R, as shown in Figure 1-29.

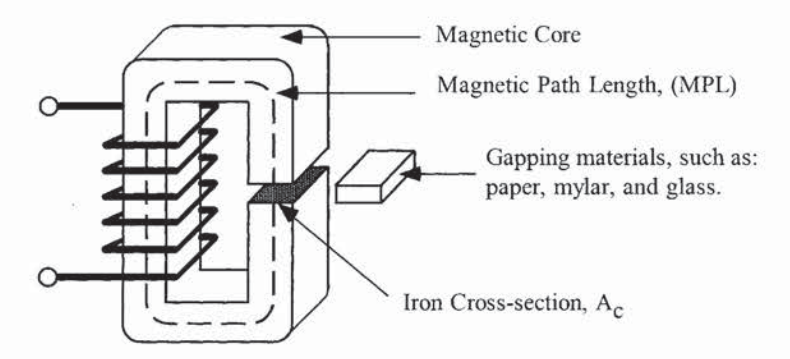


Figure 1-29. Placement of the Gapping Materials.

Placement of the gapping material is critical in keeping the core structurally balanced. If the gap is not proportioned in each leg, then the core will become unbalanced and create even more than the required gap. There are designs where it is important to place the gap in an area to minimize the noise that is caused by the fringing flux at the gap. The gap placement for different core configurations is shown in Figure 1-30. The standard gap placement is shown in Figure 1-30A, C, and D. The EE or EC cores shown in Figure 1-30B, are best-suited, when the gap has to be isolated within the magnetic assembly to minimize fringing flux noise. When the gap is used as shown in Figure 1-30A, C, and D, then, only half the thickness of the calculated gap dimension is used in each leg of the core.

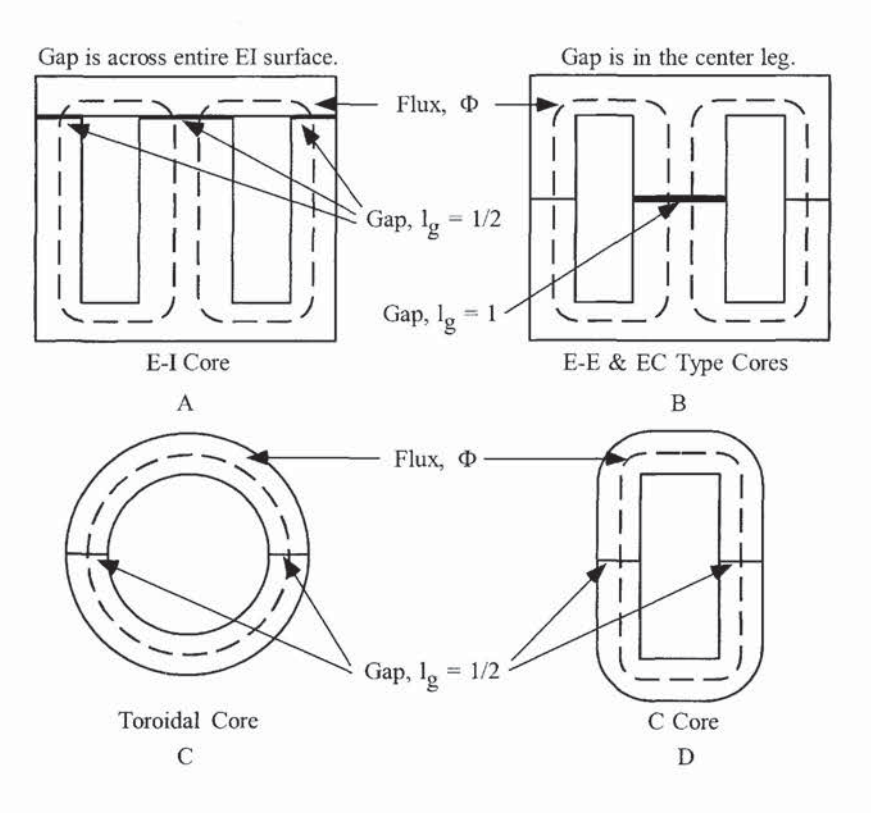


Figure 1-30. Gap Placement using Different Core Configurations.

Fringing Flux

Introduction

Fringing flux has been around since time began for the power conversion engineer. Designing power conversion magnetics that produce a minimum of fringing flux has always been a problem. Engineers have learned to design around fringing flux, and minimize its effects. It seems that when engineers do have a problem, it is usually at the time when the design is finished and ready to go. It is then that the engineer will observe something that was not recognized before. This happens during the final test when the unit becomes unstable, the inductor current is nonlinear, or the engineer just located a hot spot during testing. Fringing flux can cause a multitude of problems. Fringing flux can reduce the overall efficiency of the converter, by generating eddy currents that cause localized heating in the windings and/or the brackets. When designing inductors, fringing flux must to be taken into consideration. If the fringing flux is not handled correctly, there will be premature core saturation. More and more magnetic components are now designed to operate in the sub-megahertz region. High frequency has really brought out the fringing flux and its parasitic eddy currents. Operating at high frequency has made the engineer very much aware of what fringing flux can do to hamper a design.

Material Permeability, (μm)

The B-H loops that are normally seen in the manufacturers' catalogs are usually taken from a toroidal sample of the magnetic material. The toroidal core, without a gap, is the ideal shape to view the B-H loop of a given material. The material permeability, $u_{\rm m}$, will be seen at its highest in the toroidal shape, as shown in Figure 1-31.

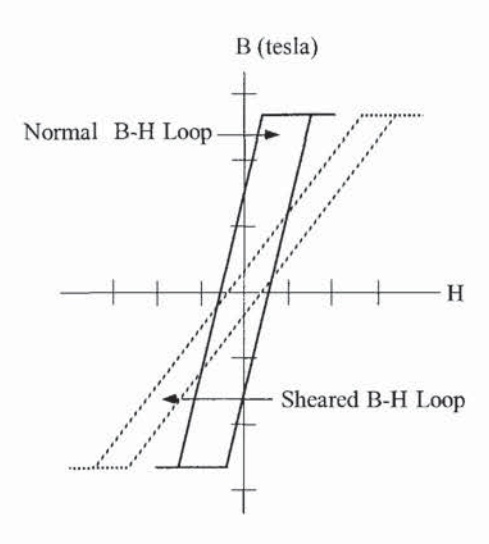


Figure 1-31. The Shearing of an Idealized B-H Loop Due to an Air Gap.

A small amount of air gap, less than 25 microns, has a powerful effect by shearing over the B-H loop. This shearing over of the B-H loop reduces the permeability. High permeability ferrites that are cut, like E cores, have only about 80 percent of the permeability, than that of a toroid of the same material. This is because of the induced gap, even though the mating surfaces are highly polished. In general, magnetic materials with high-permeability, are sensitive to temperature, pressure, exciting voltage, and frequency. The inductance change is directly proportional to the permeability change. This change in inductance will have an effect on the exciting current. It is very easy to see, that inductors that are designed into an LC, tuned circuit, must have a stable permeability, u_e.

$$L = \frac{0.4\pi N^2 A_c \Delta \mu (10^{-8})}{\text{MPL}}, \text{ [henrys] [1-32]}$$

Air Gaps

Air gaps are introduced into magnetic cores for a variety of reasons. In a transformer design a small air gap, l_g , inserted into the magnetic path, will lower and stabilize the effective permeability, μ_e .

$$\mu_e = \frac{\mu_m}{1 + \mu_m \left(\frac{l_g}{\text{MPL}}\right)}$$
 [1-33]

This will result in a tighter control of the permeability change with temperature, and exciting voltage. Inductor designs will normally require a large air gap, l_g , to handle the dc flux.

$$l_g = \frac{0.4\pi N I_{dc} (10^{-4})}{B_{dc}}, \text{ [cm] [1-34]}$$

Whenever an air gap is inserted into the magnetic path, as shown in Figure 1-32, there is an induced, fringing flux at the gap.

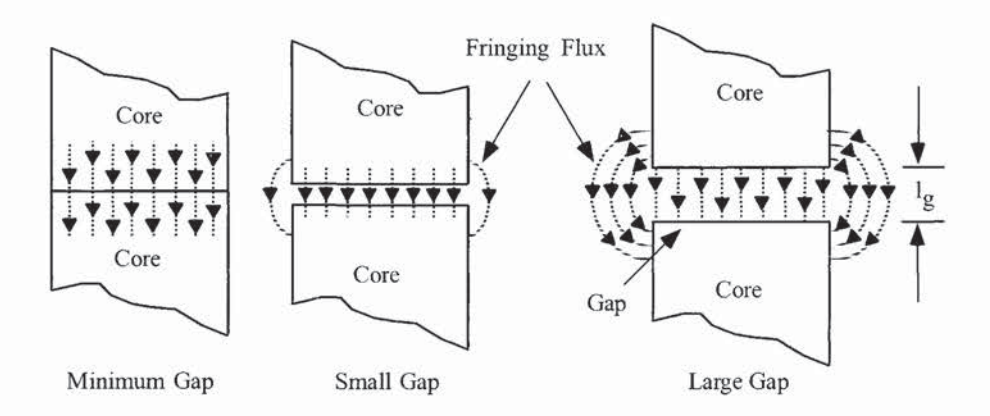


Figure 1-32. Fringing Flux at the Gap.

The fringing flux effect is a function of gap dimension, the shape of the pole faces, and the shape, size, and location of the winding. Its net effect is to shorten the air gap. Fringing flux decreases the total reluctance of the magnetic path and, therefore, increases the inductance by a factor, F, to a value greater than the one calculated.

Fringing Flux, F

Fringing flux is completely around the gap and re-enters the core in a direction of high loss, as shown in Figure 1-33. Accurate prediction of gap loss, P_g, created by fringing flux is very difficult to calculate.

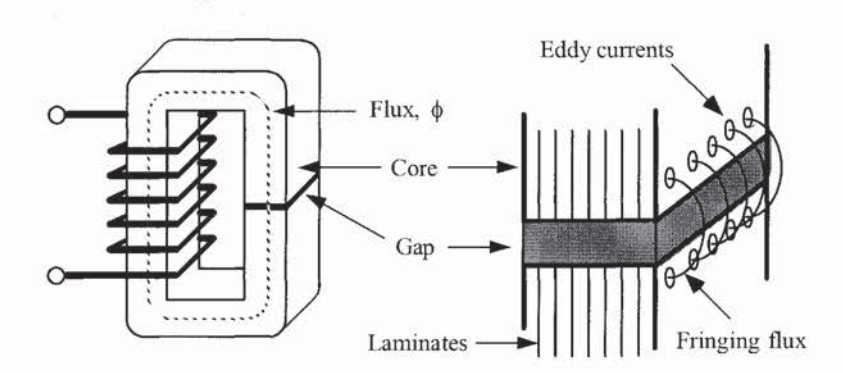


Figure 1-33. Fringing Flux, with High Loss Eddy Currents.

This area around the gap is very sensitive to metal objects, such as clamps, brackets and banding materials. The sensitivity is dependent on the intensity of the magnetomotive force, gap dimensions and the operating frequency. If a metal bracket or banding material is used to secure the core, and it passes over the gap, two things can happen: (1) If the material ferromagnetic is placed over the gap, or is in close proximity so it conducts the magnetic field, this is called "shorting the gap." Shorting the gap is the same as reducing the gap dimension, thereby producing a higher inductance, than designed, and could drive the core into saturation. (2) If the material is metallic, (such as copper, or phosphor bronze), but not ferromagnetic, it will not short the gap or change the inductance. In both cases, if the fringing flux is strong enough, it will induce eddy currents that will cause localized heating. This is the same principle used in induction heating.

Gapped, dc Inductor Design

The fringing flux factor, F, has an impact on the basic inductor design equations. When the engineer starts a design, he or she must determine the maximum values for B_{dc} and for B_{ac} , which will not produce magnetic saturation. The magnetic material that has been selected will dictate the saturation flux density. The basic equation for maximum flux density is:

$$B_{\text{max}} = \frac{0.4\pi N \left(I_{dc} + \frac{\Delta I}{2} \right) (10^{-4})}{I_g + \frac{\text{MPL}}{\mu_m}}, \text{ [tesla]} \quad [1-35]$$

The inductance of an iron-core inductor, carrying dc and having an air gap, may be expressed as:

$$L = \frac{0.4\pi N^2 A_c \left(10^{-8}\right)}{l_g + \frac{\text{MPL}}{\mu_m}}, \text{ [henrys]} \quad [1-36]$$

The inductance is dependent on the effective length of the magnetic path, which is the sum of the air gap length, l_g , and the ratio of the core magnetic path length to the material permeability, (MPL/ u_m). The final determination of the air gap size requires consideration of the fringing flux effect which is a function of the

gap dimension, the shape of the pole faces, and the shape, size, and location of the winding. The winding length, or the G dimension of the core, has a big influence on the fringing flux. See, Figure 1-34 and Equation 1-37.

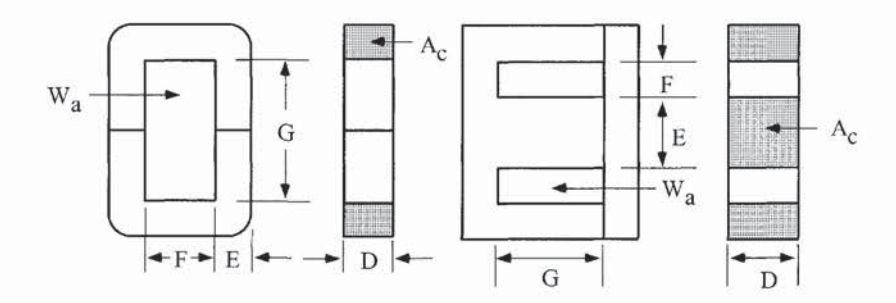


Figure 1-34. Dimensional, Call Out for C and E Cores.

The fringing flux decreases the total reluctance of the magnetic path length and, therefore, increases the inductance by a factor of F to a value greater than that calculated. The fringing flux factor is:

$$F = \left(1 + \frac{l_g}{\sqrt{A_c}} \ln \frac{2G}{l_g}\right) \quad [1-37]$$

After the inductance has been calculated using Equation 1-36, the fringing flux factor has to be incorporated into Equation 1-36. Equation 1-36 can now be rewritten to include the fringing flux factor, as shown:

$$L = F \left(\frac{0.4\pi N^2 A_c \left(10^{-8} \right)}{I_g + \frac{\text{MPL}}{\mu_m}} \right), \text{ [henrys] [1-38]}$$

The fringing flux factor, F, can now be included into Equation 1-35. This will check for premature, core saturation.

$$B_{\text{max}} = F \left(\frac{0.4\pi N \left(I_{de} + \frac{\Delta I}{2} \right) \left(10^{-4} \right)}{I_g + \frac{\text{MPL}}{\mu_{\text{m}}}} \right), \text{ [tesla] [1-39]}$$

Now that the fringing flux factor, F, is known and inserted into Equation 1-38. Equation 1-38 can be rewritten to solve for the required turns so that premature core saturation will not happen.

$$N = \sqrt{\frac{L\left(l_g + \frac{\text{MPL}}{\mu_m}\right)}{0.4\pi A_c F\left(10^{-8}\right)}}, \text{ [turns] [1-40]}$$

Fringing Flux and Coil Proximity

As the air gap increases, the fringing flux will increase. Fringing flux will fringe out away from the gap by the distance of the gap. If a coil was wound tightly around the core and encompasses the gap, the flux generated around the magnet wire will force the fringing flux back into the core. The end result will not produce any fringing flux at all, as shown in Figure 1-35. As the coil distance moves away from the core, the fringing flux will increase until the coil distance from the core is equal to the gap dimension.

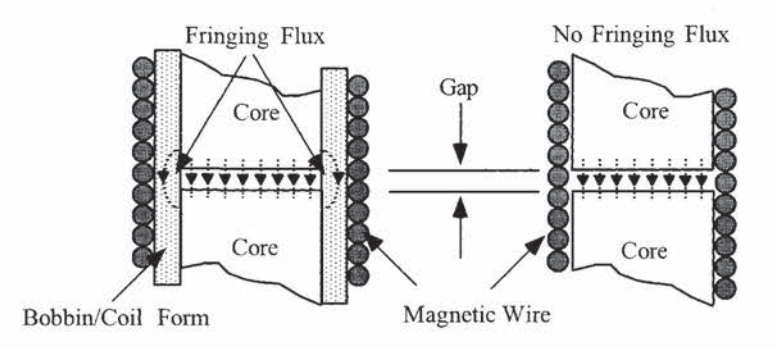


Figure 1-35. Comparing a Tightly-Wound Coil, and a Coil Wound on a Coil Form.

Fringing Flux, Crowding

Flux will always take the path of highest permeability. This can best be seen in transformers with interleave laminations. The flux will traverse along the lamination until it meets its mating, I or E. At this point, the flux will jump to the adjacent lamination and bypass the mating point, as shown in Figure 1-36.

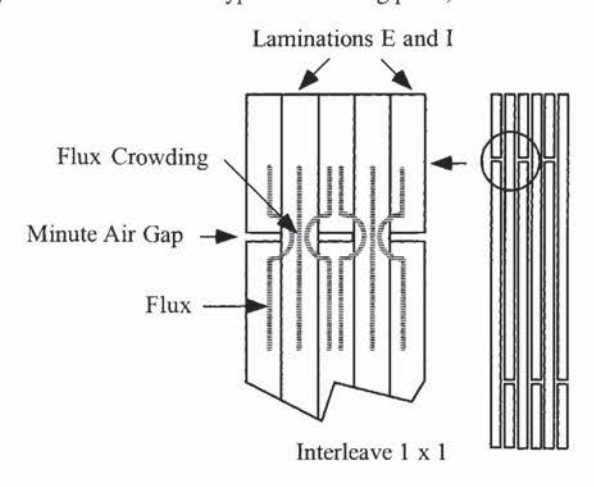


Figure 1-36. Flux Crowding in Adjacent Laminations.

This phenomena can best be seen by observing the exciting current at low, medium and high flux levels, as shown in Figure 1-37. At low levels of excitation, the exciting current is almost square, due to the flux taking the high permeability path, by jumping to the adjacent lamination, as shown in Figure 1-36. As the excitation is increased, the adjoining lamination will start to saturate, and the exciting current will increase and become nonlinear. When the adjacent lamination approaches saturation, the permeability drops. It is then that the flux will go in a straight line and cross the minute air gap, as shown in Figure 1-36.

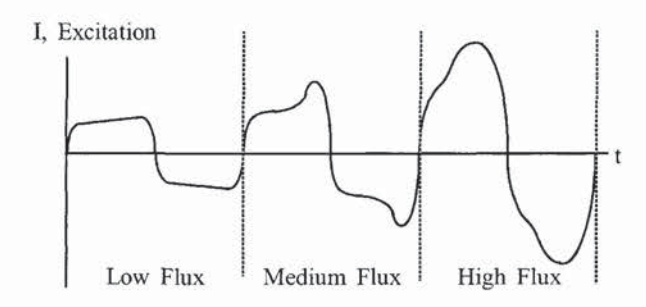


Figure 1-37. Exciting Current, at Different Levels of Flux Density, B.

Fringing Flux and Powder Cores

Designing high frequency converters, using low permeability powder cores, will usually require very few turns. Low perm power cores (less than 60), exhibit fringing flux. Powder cores with a distributed gap will have fringing flux that shorts the gap and gives the impression of a core with a higher permeability. Because of the fringing flux and a few turns, it is very important to wind uniformly and in a consistent manner. This winding is done to control the fringing flux and get inductance repeatability from one core to another, as shown in Figures 1-38 and 1-39.

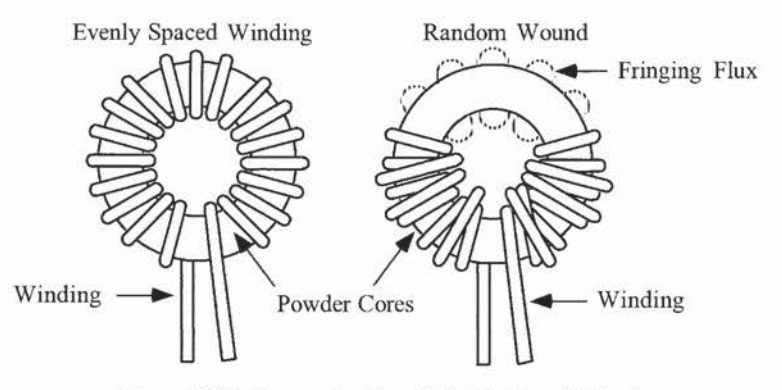


Figure 1-38. Comparing Toroidal, Winding Methods.

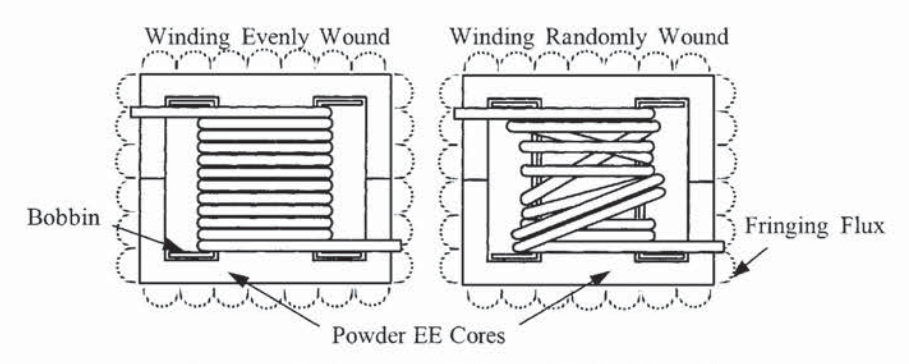


Figure 1-39. Comparing EE Cores, Winding Methods.